Journal of the Meteorological Society of Japan

EARLY ONLINE RELEASE

The DOI for this manuscript is
DOI:10.2151/jmsj.2025-022
J-STAGE Advance published date: March 17, 2025

Generation of ensemble perturbations using low-precision floating-point numbers

Tsuyoshi Yamaura[1]

RIKEN Center for Computational Science, Kobe, JAPAN

March 3, 2025

----

1) Corresponding author: Tsuyoshi Yamaura, RIKEN Center for Computational Science, 7-1-26, Minatojima-minami-machi, Chuo-ku, Kobe, Hyogo 650-0047, JAPAN
E-mail: tyamaura@riken.jp
Tel: +81-78-940-5730

Abstract

The objective of this study is to improve forecast accuracy by using low-precision floating-point arithmetic when performing ensemble weather forecasting. Low-precision floating-point arithmetic is reproduced using a software emulator developed to allow the mantissa bit length of floating-point numbers to be adjusted in one-bit increments. First, two different methods of generating an ensemble forecast using low-precision techniques were compared with a conventional ensemble-generation approach. For one, the precision of the initial conditions is reduced (called initial value ensemble), and for the other, the precision of the model calculations is reduced (called model ensemble). Then, it is found that the former technique is inadequate for generating sufficient ensemble spread, but the latter gives an ensemble spread comparable to the reference. In order to further evaluate the ensemble method using low-precision floating-point arithmetic in accordance with the model ensemble method, ensemble forecasting experiments were conducted in combination with the conventional ensemble method. As a result, the combined ensemble forecast had a higher spread evaluation index than the ensemble forecast using only the low-precision floating-point arithmetic and the conventional ensemble method. The reasons why the ensemble forecasts have higher index when incorporating low-precision floating-point ensemble methods are considered as follows: weather forecast models do not reproduce weather phenomena below the grid scale due

to their low spatio-temporal resolution, and some models incorporate statistical assumptions to reduce computational load, which suppress the random nature of weather phenomena rather than actual weather events. On the other hand, ensemble methods using low-precision floating-point arithmetic can compensate for this randomness, and thus are expected to have higher evaluation index. This suggests that low-precision floating-point arithmetic, implemented in hardware by using Field Programmable Gate-Arrays (FPGAs) for example, may allow for faster operations without compromising forecast accuracy in ensemble forecasting.

Keywords HPC; inexact computing; low-precision floating point numbers; ensemble weather forecasting

1. Introduction

Recently, a numerical weather model is an application that requires both huge data and computational performance. Saving computational costs becomes a critical issue to the weather forecasting model. One of the methods for saving cost is to reduce the precision of a simulation, which is called inexact computing (Lingamneni et al. 2011). Prior research has investigated how to enable operations with reduced precision while taking into account bit errors associated with power savings and the errors caused by reducing the precision of operations. Inexact computing is essential for future high-performance computing (HPC) systems.

One of the methods of inexact computing is to reduce the precision of floating-point operations, i.e., to use low-precision floating-point numbers, such as single-precision floating-point numbers, to perform operations that are conventionally performed using double-precision floating-point numbers in numerical weather models. This method has already been used in various numerical weather models. For example, the Weather Research and Forecasting (WRF) model developed by the National Center for Atmospheric Research (NCAR) incorporates single-precision floating-point arithmetic into atmospheric model calculations. Mielikainen et al. (2012) switched to single-precision floating-point arithmetic when using a Graphic Processing Unit (GPU) accelerator and succeeded in accelerating the radiation model. Similarly, the Integrated Forecasting System (IFS) developed by the European Centre for Medium-Range Weather Forecasts (ECMWF) has changed almost all variables used in weather forecasting from double-precision floating-point numbers to single-precision floating-point numbers, improving total wall clock time by 40% while not significantly degrading forecast accuracy (Vàňa et al. 2017). The Non-hydrostatic Icosahederal Atmospheric Model (NICAM) also performs single-precision floating-point calculations to improve computational speed with little impact on computational accuracy (Nakano et al. 2018). In addition to other numerical models, an ocean model can also perform single-precision floating-point operations (Yamagishi and Matsumura 2016). They succeeded in using a GPU to perform mixed-precision calculations for ocean models, and achieved a 4.7-time improvement in execution speed over using only a CPU.

Previous studies have used complex models such as those used for weather forecasting, and it was unclear how much error could be introduced into these single-precision floating-point calculations. Yamaura et al. (2019) theoretically calculated the magnitude of the rounding error that enters when the precision of floating-point operations is reduced and demonstrated it in a shallow water model. The point of that paper is that the rounding error behaves like a stochastic forcing term in the difference equation. This is an error that must occur in floating-point operations, and that if it accumulates, even mathematically stable solutions such as the geostrophic wind balance may diverge. Such errors may impact the numerical accuracy of a model simulation. But in the weather forecasting area, ensemble simulations provide an environment in which errors may be tolerated. Floating-point errors may even be beneficial for the purposes of ensemble forecasting. According to the report of Japan Meteorological Agency (JMA), there are two ways to create ensemble members for ensemble forecasts (JMA 2016): one is to create individual ensemble members independently, and the other is to create ensemble members by giving perturbations (Table 1). Each of these methods can be divided into three types: initial value ensemble, model ensemble, and boundary value ensemble, for a total of six methods. Give perturbations are mainly used for ensemble forecasting, especially for initial value ensemble methods. Local Ensemble Transform Kalman Filter (LETKF) is an extension of the Kalman filter, which combines observational data and model predictions to perform state estimation. It introduces initial perturbations according to the analysis error using a data assimilation method. Breeding Growth Mode (BGM) is given an appropriate disturbance in its initial state, and then allowed to evolve over time using the model. At this point, the growth of the perturbation is analyzed, and the perturbation is normalized at regular intervals to return the amplitude of the perturbation to its original size. This is then repeated to extract the main growth modes in the system. Singular Vector (SV) is a method for identifying the perturbation that causes the most efficient growth of the prediction error in the system. It analyzes how the initial perturbation evolves over time using linear approximation, and then adds the perturbation that grows the most. These methods create ensemble members by adding small disturbances to a certain initial state. On the other hand, there is also a method of adding perturbations during the time evolution of the model. Stochastically Perturbed

Parametrisation Tendencies (SPPT) aims to reflect the uncertainty of predictions by probabilistically representing the model errors associated with physical processes, and Stochastic Kinetic Energy Backscatter (SKEB) aims to reproduce the kinetic energy dissipated at the sub-grid scale. Sea Surface Temperature (SST) perturbation, a typical boundary value ensemble, is mainly used for long-term forecasts such as future climate predictions. It is less commonly used for short-term weather forecasting. When using floating-point arithmetic errors as an ensemble method, both initial value ensemble and model ensemble methods can be performed. In that case, which is more appropriate?

This study aims to answer the following two questions: (1) Is it possible to use the stochastic forcing that occurs when manipulating the mantissa bit length, as shown in Yamaura et al. (2019), in performing ensemble forecasting, and (2) if so, how can we use them efficiently? Reducing the precision of floating-point calculations is already being done at operational centers for weather forecasting (Rüdisühli et al. 2014, Lang et al. 2021), and this is done solely with the aim of reducing execution time. This research investigates the possibility of not only reducing execution time, but also improving the physical performance of ensemble forecasting. This paper is organized as follows. Section 2 describes the data used, numerical models, and experimental methods. Section 3 presents the experimental results. Section 4 describes a discussion of the results, and Section 5 presents a summary.

2. Data and Method

This study adopts the regional model (RM) version 5.4.5 with the Scalable Computing for Advanced Library and Environment (SCALE), which is a weather infrastructure library developed and published by RIKEN (Nishizawa et al. 2015, Sato et al. 2015). SCALE-RM is a proven model that has already been used in many studies, not only for climate research applications but also as a weather forecasting model (Adachi et al. 2019, Honda et al. 2022a, b, Sueki et al. 2022, and Miyoshi et al. 2023). Initial values are created using the normal procedures implemented in SCALE-RM. SCALE-RM first reads in terrain and land use data from an external source (e.g., Global Land Cover Characteristics Data Base Version 2.0 (GLCCv2) and Global 30 Arc-Second Elevation (GTOPO30) provided by U.S. Geological Survey) and interpolates it to the grid point coordinates in the computational domain. To create initial and boundary values, this topography and land use data is read in and the data set used for initial and boundary values is interpolated in the same way. Data that are important as forecast variables but not included in the objective analysis data set (e.g., atmospheric density) are calculated in the SCALE-RM initial value generation process using formulas that follow physics law. In the case of atmospheric density, calculations are performed assuming hydrostatic equilibrium.

To achieve arbitrary floating-point precision in this SCALE-RM, an emulator that rounds the bit length of the mantissa part was introduced. The emulator performs an operation to round the mantissa bits of floating-point numbers with sufficiently long mantissa bits to an arbitrary length for each operation. This rounding is based on the nearest-even rounding specified in IEEE754, which can reproduce the floating-point arithmetic precision of the specified bit as long as the exponent bit does not overflow. This study uses this emulator to adjust the precision of floating-point operations at the software level. Specifically, the following is done: In the initial value ensemble method, the precision of the prognostic variables is reduced just before they are output to the file as initial and boundary data. On the other hand, in the case of the model ensemble method, the precision of the prognostic variables is reduced during the forecast calculation. SCALE-RM is divided into two modules: the dynamics module, which performs calculations based on geophysical fluid dynamics, and the physics module, which handles other physical processes. The physics module consists of six modules: turbulence closure, radiation, cloud microphysics, cumulus parameters, boundary layer, and surface modules. In each of these modules, an operation to shorten the mantissa bit lengths is implemented by overloading the operators and built-in functions for the prognostic variables so that the calculation does not break down by the emulation. And then, the precision of the calculation is reduced to an arbitrary level. Since this study is intended for short-term weather forecasting, the boundary value ensemble method is excluded.

This paragraph describes the settings that are common throughout the experiment. The computational domain for the SCALE-RM is shown in Figure 1. The computational domain is large enough to capture general synoptic-scale meteorological phenomena near Japan. The horizontal resolution is 18 km, the vertical layer is 40 layers, the time interval of one model step is 30 seconds, and the integration period is 5 days. Ensemble member data (EPSW) included in the JMA grid point value (JMA-GPV) dataset was employed to conduct the ensemble forecast experiments. This three-dimensional data includes three layers of 850, 500, and 300 hPa for geopotential height, temperature, zonal winds, meridional winds, and relative humidity. As this data was insufficient for the vertical layer, SCALE-RM could not be run properly. So objective analysis values provided by JMA for other layers were adopted for the same time period. The two-dimensional data include surface pressure, mean sea level pressure, 10-meter-high zonal winds, 10-meter-high meridional winds, 2-meter-high temperature, and 2-meter-high relative humidity. A total of 27 members were distributed for these ensemble data, ranging from -13 to +13 based on 0. This was used to create the initial and boundary data for the ensemble experiments in SCALE-RM. In this study, the ensemble experiment using only this EPSW data is referred to as a conventional ensemble method and will be used as a comparison for evaluating ensemble methods with rounding errors. Other settings that vary from experiment to experiment are described in the later sections.

3. Results

In this section, ensemble experiments will be conducted using emulators with arbitrarily adjustable precision, and the potential application of rounding errors to ensemble experiments will be examined. There are two types of ensemble experiments conducted in this study: first, a comparison is made between the initial value ensemble condition and the model ensemble condition. Second, ensemble experiments with rounding errors in the dynamics and physics modules of SCALE-RM will be conducted.

3.1 Comparing Initial value ensemble method with model ensemble method

First, to ascertain the effect of rounding errors in the initial and model ensembles, the following two types of experiments are compared: an experiment in which calculations are performed using initial value data with reduced mantissa bit lengths (Init-run), and an experiment in which calculations are performed using the same initial value data with reduced mantissa bit lengths within the model calculations (FPN-run). Next, the ensemble forecast experiment to be performed is described. Ensemble member 0 performs the calculation using double-precision floating-point numbers (mantissa bit length: 52 bits) as is. Ensemble members 1 through 8 are double-precision floating-point numbers with reduced mantissa bit lengths of 45, 40, 35, 30, 25, 20, 15, and 10 bits. 10 bits corresponds to a half-precision floating-point number. The reduction in precision is applied only to the initial conditions in the Init-run, and is performed during the model calculation in the FPN-run. For comparison, I also perform an experiment (EPSW-run) using ensemble members produced by the JMA. The JMA ensemble data uses SV as a method for creating initial perturbations, and it is mainly used to efficiently express the uncertainty of the model with a small number of members. The SV is a method for calculating perturbations with large linear growth rates in the specified evaluation time and area, and it is one of the effective initial perturbation creation methods for ensemble forecasts. Let's represent the state of the atmosphere as an n-dimensional column vector X. The components of this vector are things like the temperature and wind speed at each location. If we define the function M as taking the initial value X_0 at time 0 and outputting the forecast value X_t at time t, then numerical weather prediction can be expressed formally as $X_t = M(X_0)$. In this equation, if we consider the change in the forecast value X'_t for the initial perturbation X'_0, the relationship between the two is as follows,

$$X'_t = M\left(X_0 + X'_0\right) - M(X_0) \simeq \frac{\partial M}{\partial X_0} X'_0 \equiv \boldsymbol{M} X'_0.$$

Here, $M\left(X_0 + X'_0\right)$ is expanded in Taylor series and the higher-order terms of X'_0 are ignored, and then X'_t and X'_0 are linearly connected. The $\partial M / \partial X_0$ that appears in this formula is a square matrix of order n, which is composed of partial derivatives of the components of M with respect to the components of X_0, and is called a linear operator. This matrix is represented by $\boldsymbol{M}$. The magnitude of the change in the initial and forecast values is defined by the norm, $\|X'\| = \sqrt{(X' \cdot X')}$, where the appropriate inner product is used, and the one with a large value of $\|X'_t\| / \|X'_0\|$ is considered to be a change with high sensitivity. This maximum value problem is obtained by SV decomposition of the matrix $\boldsymbol{M}$. The first SV, second SV, etc. are called in order of high sensitivity, and these correspond to the ensemble members.

The date of this initial condition is October 15, 2019 (Figure 2). At this time, there is a typical low-pressure system and front near Japan, which is a good sample for mid-latitude weather forecasting. Compared to the EPSW-run results (Figs. 3a, d, and g), the Init-run results show very little variability even after 5 days of integration (Figs. 3b, e, and h). This indicates that even if rounding errors are mixed in the initial values, they have little effect on the ensemble forecast results. Although the precision of half-precision floating-point numbers has only about three decimal places, it suggests that even if the initial value contains this level of error, it will not result in an ensemble forecast with sufficient spread.

Why is there so little variation even if the initial value contains an error of the magnitude of a half-precision floating-point operation? It is due to the nature of rounding errors. Figure 4 shows the frequency distribution of rounding error in the geostrophic wind equilibrium experiment conducted by Yamaura et al. (2019). They showed that the error grows even when given a geostrophic wind parameter that is mathematically in equilibrium. The frequency distribution of the rounding error was examined and found to be Gaussian. This can be explained by the central limit theorem, where the random variable follows a Gaussian distribution. It is shown that each rounding error is not determined by probability, but the set of errors behaves in a probabilistic manner. However, once an error with such a behavior is given as an initial value, it is not appropriate as an ensemble member. In a meteorological field, not just any wave will grow, but there are modes that are more likely to grow. For example, the BGM method, one of the initial value ensemble methods, creates ensemble members by inserting such growth-prone waves. To create a meaningful ensemble member with noise such as a Gaussian distribution requires a huge number of members. For this reason, the application of rounding error to initial value ensemble would not be suitable.

On the other hand, the FPN-run results (Figs 3c, f, and i) show less variation than the results of the EPSW-run experiment, but more variation than the Init-run results. At the initial time, there is naturally no difference among the members of the FPN-run, since no operation is performed. After 2 days, there is a visible error, and after 5 days, the western edge of the Pacific High is still wavy. However, there are few contours that show large changes, and some of the fluctuations are small, suggesting that small rounding errors do not result in large fluctuations. To confirm this, the Root Mean Square Error (RMSE) of the geopotential height at 500 hPa at 5 days after the EPSW-run, Init-run, and FPN-run are shown for each member from 1 to 8 (Fig. 5). EPSW-run varies from member to member, but it is about 10 gpm. The FPN-run is almost zero for members 1 to 6, about 2 gpm for member 7, and about 14 gpm for member 8. This means that the RMSE of the FPN-run is about 20% of the EPSW-run when the bit length of the mantissa part is limited to 15 bits, and the RMSE is about the same as the EPSW-run when the bit length is limited to 10 bits. This can be interpreted as the result of rounding errors added by floating-point arithmetic, which expanded the errors to the extent that they changed the geopotential height contours at 500 hPa. For the purpose of creating ensemble members by rounding errors, the model ensemble method is likely to be more suitable than the initial value ensemble method. Even from the perspective of calculation cost, the process of creating initial and boundary values is less demanding than the process of model prediction calculation. For this reason, FPN-run is likely to lead to a reduction in calculation cost compared to Init-run. This FPN-run is examined in more detail in the next subsection. In addition, the temperature and water vapor at the 850 hPa and the wind in the upper levels were also investigated in the same way, but the conclusion is the same as for geopotential height (figure not shown).

3.2 Pursuit of model ensemble method

The results of the previous subsection indicate that the model ensemble method may be more suitable than the initial value ensemble method for creating ensemble members using rounding errors. In this subsection, I will analyze this model ensemble method in more detail by conducting the following ensemble experiments: (1) Ensemble experiments using EPSW dataset (EPSW-run), (2) Ensemble experiments using rounding errors (FPN-run), and (3) Ensemble experiments combining (1) and (2) (Comb-run). Here, ensemble member 0 of the JMA EPSW is commonly used in all experiments, which are control experiments without adjusting the precision of the floating-point number operations. In (1), experiments are conducted using ensemble members from -12 to +12 of the EPSW ensemble members created by the JMA. There are also -13 and +13 members distributed, but I only use members -12 to +12 so that 24 members in total are considered, consistent with experiments (2) and (3). In (2), as in the previous section, an ensemble experiment is performed using only the rounding error from the model ensemble method. However, it was found that the rounding error is not very effective unless it is as large as a half-precision floating-point number, so the ensemble members were created as follows: Since SCALE-RM can be roughly divided into six physical schemes, seven members are created with rounding errors in the dynamics scheme and in each of the six physical schemes. In addition, a member that introduces rounding errors in all of them is created. In total, 8 types of members are obtained. To further increase the number of ensemble members, three types of mantissa bits are set: 11-bit, 10-bit, and 9-bit. In other words, this corresponds to conducting 24 different ensemble forecast experiments. All initial and boundary values are the same as for ensemble member 0. The following is the basis for choosing this configuration. First, I calculated the RMSE using the same method as in Figure 5, and confirmed that the values were close to the results obtained by the EPSW-run model. When the number of bits in the mantissa was 11-, 10-, and 9-bit, the RMSE obtained was 9.23, 14.04, and 25.71, respectively. Since the RMSE of EPSW-run is around 8, I judged that a sufficiently large disturbance was given. In the case where the operation of reducing the mantissa bit lengths was applied to each module individually, the average RMSE values were 2.34, 2.86, and 4.75 for 11-, 10-, and 9-bit, respectively. The RMSE values tended to be smaller than when applied to all modules, but they were larger than or equal to the RMSE of member 7 in Figure 5. Therefore, it was judged that it could be adopted as an ensemble member. Experiment (3) combines the methods in (1) and (2) and uses different data for initial and boundary values for each ensemble member, as in EPSW-run. The combination experiments are conducted using the same 24 different settings that adjust mantissa bit lengths of the floating-point number mentioned above.

Figure 6 shows the horizontal distribution of geopotential heights on the 500 hPa for the 5-day integrated ensemble forecast experiment starting at 00 UTC on October 15, 2019. The contours show the results of the objective analysis values from JMA-GPV data at that time. The shading indicates the difference from the objective analysis value of the ensemble mean. At first glance, it can be seen that none of the figures deviate significantly from the objective analysis values, indicating that the calculations were successful. At the initial time (Figs 6a, b, and c), the RMSE of the ensemble mean from the objective analysis values is almost the same for the EPSW-run, FPN-run, and Comb-run, and the ensemble spread (SPRD), which is calculated as the RMS distance from the ensemble mean, is zero for the FPN-run only. This is not surprising for the FPN-run, where there is no variation at the initial time in the experimental setup. Two days after the start of time integration (Figs. 6d, e, f), RMSE does not differ significantly among the three experiments, while SPRD shows differences. In this experiment, the EPSW-run has the smallest SPRD, followed by the FPN-run, and the Comb-run has the largest SPRD. This trend continues 5 days after the start of time integration (Figs. 6g, h, and i), with the EPSW-run having the smallest SPRD and the Comb-run having the largest SPRD. It is obvious that a small RMSE is desirable, but what about SPRD? According to Takano (2002), SPRD tends to be underestimated in ensemble forecasts of numerical weather forecast models. In other words, a large SPRD tends to be desirable for ensemble forecasting. Here, Comb-run is the most favorable result.

Figure 7 shows the horizontal distribution of temperature on the 850 hPa. As in Fig. 6, the contours show the objective analysis values at that time, and the shading indicates the deviation of the ensemble mean from the objective analysis values. The temperature in the lower troposphere is qualitatively similar to the change in geopotential height on the 500 hPa, with a tendency for improved SPRD and slightly smaller RMSE for Comb-run compared to EPSW-run. This result indicates that the rounding error by Comb-run affects not only the mid-troposphere but also the lower troposphere.

Figure 8 shows the horizontal distribution of zonal wind speeds on the 300 hPa. As in Figs. 6 and 7, the contours indicate the objective analysis values at that time, and the shading indicates the deviation from the objective analysis values of the ensemble mean. In the three experiments, there is also little qualitative change in the upper tropospheric zonal wind speeds. However, there is a difference compared to Figs. 6 and 7. Compared to the EPSW-run, the FPN-run results show a smaller SPRD, meaning that the variation due to the growth of rounding errors is smaller than the variation due to the conventional ensemble method. This suggests that the growth of rounding errors is not necessarily larger than the variation by the conventional ensemble method, but depends on the experimental setting and other factors. On the other hand, Comb-run has a larger value of SPRD and a smaller value of RMSE than the other two. This indicates that in ensemble forecasts, rounding error works in the direction of improving the conventional ensemble method in all troposphere.

The results in Figures 6 through 8 are for only one case, starting on October 15, 2019; it is not clear if the general result is that the Comb-run results have a smaller RMSE and larger

SPRD than the EPSW-run. It is also clear that the closer the RMSE is to zero, the better the forecast performance, but it is not obvious what spread of SPRD is optimal. Therefore, we will increase the number of ensemble forecasting cases and introduce a measure that can objectively evaluate the spread of the ensemble spread from the set of forecast results. The Spread Evaluation Index (R) by Takano (2002) is as follows:

$$R = \frac{(M+1)\langle S^2 \rangle}{(M-1)\langle E_M^2 \rangle},$$

where M is the number of ensemble members, S is the ensemble spread, E_M is the ensemble mean of RMSE, and the angle brackets mean multiple-case average treatment. The closer R is to 1, the more reasonable the size of the ensemble spread is; greater than 1 means the ensemble spread is oversized, and less than 1 means the ensemble spread is undersized.

Figure 9 shows the time evolution of the Spread Evaluation Index evaluated in terms of geopotential height at 500 hPa from the start to the end of time integration for 24 cases with initial values at 00 UTC on the 1st and 15th of each month in 2019. The horizontal axis indicates elapsed time and the vertical axis indicates the magnitude of Spread Evaluation Index. In all cases, the magnitude of the Index is less than 1, indicating that the ensemble spread is underestimated. In general, ensemble spread tends to be underestimated in ensemble forecasts, and R becomes smaller than 1 (Takano 2002). Long-term weather forecasts by ECMWF underestimate the ensemble spread over several years, and short-term weather forecasts by JMA intentionally overestimate the ensemble spread at the initial time in anticipation of the underestimation of the ensemble spread.

In both cases, the tendency of the weather forecast models to underestimate the ensemble spread remains unchanged, and is consistent with Fig. 9 in this study: for the EPSW-run, the magnitude of the index drops immediately after the start of time integration and reaches around 0.2 after 120 hours. For FPN-run, the ensemble spread is naturally zero at the initial time, and increases after the start of integration, and remains the same or higher than EPSW-run until 60 hours, after which it falls below EPSW-run. This suggests that although the size of the ensemble spread of FPN-run is similar to that of EPSW-run immediately after the start of integration, its growth rate is not very large, and the spread becomes worse than that of conventional ensemble methods when integrated over a long period of time. The Comb-run is equal to the EPSW-run at the initial time, and thereafter the size of the index is always larger than the EPSW-run until 120 hours later. This indicates that the conventional ensemble method is improved by incorporating rounding errors. This result is for the geopotential height at 500 hPa, but similar results can be obtained with Spread Evaluation index for other variables and altitudes (figure not shown).

4. Discussion

In the previous section, we found that ensemble experiments with large rounding errors during computation give RMSEs and ensemble spread variations that are close in magnitude to those of traditional initial value ensemble methods. Furthermore, it was found that the combination of the methods can obtain a larger variance compared with the conventional initial value ensemble method. This section discusses three points: why adding rounding errors improves RMSE and ensemble spread variation, what the physical implications are when adding rounding errors, and what the advantages of rounding error ensemble methods are.

To understand why rounding errors improve ensemble forecast results, we first consider how rounding errors can be expressed. As shown in equation (1) in Yamaura et al. (2019), this can be expressed in the following form:

$$p = p^{(0)} + p^{(\varepsilon)}\,, \qquad (1)$$

where p is a variable expressed as a floating-point number on a computer, $p^{(0)}$ is the true value of the variable, and $p^{(\varepsilon)}$ is the rounding error. As can be seen from the equation, the floating-point number on the computer is expressed as the sum of the true value and the error. This is similar to the way random numbers are injected by the SPPT scheme; the format of SPPT is as follows:

$$X_p = (1 + r_X)X_c\,, \qquad (2)$$

where X_p is the variable given the perturbation, r_X is a uniformly distributed random number in the range [-0.5:0.5], and X_c is the variable before the perturbation. The SPPT scheme is related to the uncertainty in the existing parametrization scheme. This uncertainty is believed to be due to an underestimation of the subgrid-scale processes to be parametrized. Therefore, the SPPT scheme is a generalization of the existing subgrid-scale parametrization output as a probability distribution (Palmer et al. 2009). Comparing equation (2) with equation (1), it is clear that they share the same process of adding random numbers. Also, $p^{(\varepsilon)}$ is correlated with the magnitude of $p^{(0)}$, and can be regarded as one of the variables that multiplies $p^{(0)}$ by a random number. In other words, the insertion of rounding errors can be considered a type of SPPT, and since the ensemble method with rounding errors works to compensate for the effects of subgrid-scale weather phenomena, it can be combined with conventional model ensemble methods to improve forecast results.

Considering the insertion of rounding errors as a kind of SPPT scheme, it is easy to imagine that the physical implications also follow. In other words, the discretized representation of weather phenomena on computer grid points reduces the information about the original phenomena somewhat, which leads to uncertainty. Corrections with random numbers have been introduced to mitigate such subgrid-scale effects. For example, the Reynolds-Averaged Navier-Stokes equations commonly used in meteorological calculations to calculate turbulence separate the flow field into mean flow and Reynolds stress, which is the turbulence from the mean flow. In order to represent the Reynolds stress, some approximation must be made, and this approximation operation results in missing information. It is thought that the introduction of a high-resolution and high-precision scheme will reduce the missing information, but it will not be possible to prevent it completely as long as the computational resources of computers are finite. This missing information leads to an underestimation of the ensemble spread of weather calculations compared to the expected spread, and the correction by random numbers works to mitigate this. The same is true for other schemes besides turbulence.

This ensemble method of introducing rounding errors uses random numbers to introduce the effects of subgrid-scale weather phenomena. On the other hand, the method does not necessarily have to involve rounding errors. For example, you can achieve the same effect using pseudo-random numbers generated by software, but using a pseudo-random number generator requires additional computational costs. Using random numbers generated by a hardware random number generator would be less expensive, but in this case, it would be difficult to obtain reproducibility of random numbers. If the random numbers are not reproducible, it may hinder the investigation of the cause of a problem in the model. Therefore, the use of hardware random number generators is not a desirable choice. Based on these considerations, rounding errors have virtually no cost because they are generated automatically and they are reproducible. Low-precision floating-point arithmetic is also cost-effective and thus provides numerical advantages. As a result of this study, ensemble forecast calculations using mixed precision calculations with double-, single-, and half-precision are also meaningful, even if they are not arbitrary precision. In particular, the possibility of actively adopting half-precision calculations, which are often adjusted for artificial intelligence calculations, is considered to be very useful for future HPC systems. Furthermore, field programmable gate arrays (FPGAs) and other devices can be used to perform floating-point operations of various precision without loss. Rounding errors are only noise in the pursuit of deterministic solutions, but they do not interfere with numerical calculations that require probabilistic interpretation, such as ensemble forecasting, and can contribute to improved and faster calculations if used properly.

5. Summary

The purpose of this study is to determine whether the rounding errors generated by low-precision floating-point arithmetic can be used for ensemble members when making ensemble forecasts, and if so, how best to use them. Low-precision floating-point operations were reproduced using a software emulator developed to allow adjustment of the mantissa bits of floating-point numbers in one-bit increments. First, we evaluated ensemble methods based on rounding errors in accordance with both the initial value ensemble method and the model ensemble method. The rounding error ensemble method was found to be unsuitable for the initial value ensemble method because it acts like Gaussian noise and does not increase the ensemble spread very much. On the other hand, it was confirmed that the model ensemble method widens the ensemble spread to the same extent as the conventional ensemble method. This indicates that the model ensemble method is more suitable for treating rounding errors as ensemble members.

In order to further evaluate the ensemble method with rounding errors, I conducted an ensemble forecast experiment combining it with the conventional ensemble method. The results showed that the spread evaluation index was higher for the combined ensemble forecast than for the ensemble forecast using either the conventional ensemble method or the ensemble method with rounding errors alone. This suggests that the accuracy of ensemble forecasts can be improved by incorporating model ensemble methods as well as conventional ensemble methods.

The following are possible reasons why incorporating ensemble methods with low-precision floating-point arithmetic can result in higher ensemble forecast evaluation values. Weather forecast models have a lower spatio-temporal resolution than in reality, and thus are not able to reproduce weather phenomena below the grid scale. Some models incorporate statistical assumptions to reduce the computational burden, which suppress the random nature of weather phenomena more than actual weather events. On the other hand, model ensemble methods with rounding errors can compensate for this randomness. Therefore, it is expected to receive a higher rating by the Spread Evaluation Index.

The validation of this study was performed on a software emulator. This suggests that FPGAs can also be used to implement low-precision floating-point arithmetic on hardware, which may allow for faster operations in ensemble forecasts without compromising forecast accuracy. On the other hand, the problem is that it is not yet widespread to actually use an FPGA to program. When using OpenCL to use an FPGA, it is necessary to use C/C++ rather than Fortran, which has long been used in the field of fluid dynamics. That is, it is not possible to use the existing libraries for meteorological programs as they are. Therefore, the barrier to actually creating a meteorological model using an FPGA is high, and how much it can be sped up will be a future issue.

Data Availability Statement

Scalable computing for Advanced Library and Environment (SCALE) and its regional model (RM) are distributed with open-source license (https://scale.riken.jp/). However, the experimental data is very large in file size and not suitable for distribution, so contact the corresponding author.

Acknowledgments

This work was supported by JSPS KAKENHI Grant Number JP21K03663. I thank two anonymous reviewers and an associate editor for their highly constructive comments.

References

Adachi, S. A., S. Nishizawa, K. Ando, T. Yamaura, R. Yoshida, H. Yashiro, Y. Kajikawa, and H. Tomita, 2019: An evaluation method for uncertainties in regional climate projections. *Atmos. Sci. Lett.*, **20**, e877, doi:10.1002/asl.877.

Honda, T., A. Amemiya, S. Otsuka, J. Taylor, Y. Maejima, S. Nishizawa, T. Yamaura, K. Sueki, H. Tomita, and T. Miyoshi, 2022: Advantage of 30-s-updating numerical weather prediction with a phased-array weather radar over operational nowcast for a convective precipitation system. *Geophys. Res. Lett.*, **49**, e2021GL096927, doi:10.1029/2021GL096927.

Honda, T., A. Amemiya, S. Otsuka, G.-Y. Lien, J. Taylor, Y. Maejima, S. Nishizawa, T. Yamaura, K. Sueki, H. Tomita, S. Satoh, Y. Ishikawa, and T. Miyoshi, 2022: Development of the real-time 30-s-update big data assimilation system for convective rainfall prediction with a phased array weather radar: description and preliminary evaluation. *J. Adv. Model. Earth Syst.*, **14**, e2021MS002823, doi:10.1029/2021MS002823.

Japan Meteorological Agency, 2016: Challenges and prospects of ensemble forecasting for probabilistic weather forecasting. Numerical forecast section report, **62**, 1-132, https://www.jma.go.jp/jma/kishou/books/nwpreport/62/No62_all.pdf (in Japanese).

Lang, S. T. K., A. Dawson, M. Diamantakis, P. Dueben, S. Hatfield, M. Leutbecher, T. Palmer, F. Prates, C. D. Roberts, I. Sandu, and N. Wedi, 2021: More accuracy with less precision. *Q. J. R. Meteorol. Soc.*, **147**, 4358-4370, doi.org/10.1002/qj.4181.

Lingamneni, A., C. C. Enz, J.-L. Nagel, K. V. Palem, and C. Piguet, 2011: Energy parsimonious circuit design through probabilistic pruning. *Proc. of Design, Automation and Test in Europe Conference*, 764-769.

Mielikainen, J., B. Huang, H.-L. A. Huang, and M. D. Goldberg, 2012: GPU acceleration of the updated Goddard shortwave radiation scheme in the Weather Research and Forecasting (WRF) model. *IEEE Journal of selected topics in applied earth observations and remote sensing*, **5**, 555-562, doi:10.1109/JSTARS.2012.2186119.

Miyoshi, T., A. Amemiya, S. Otsuka, Y. Maejima, J. Taylor, T. Honda, H. Tomita, S. Nishizawa, K. Sueki, T. Yamaura, Y. Ishikawa, S. Satoh, T. Ushio, K. Koike, and A. Uno, 2023: Big data assimilation: Real-time 30-second-refresh heavy rain forecast using Fugaku during Tokyo Olympics and Paralympics. *Proceedings of the International Conference for High Performance Computing, Networking, Storage and Analysis*, 1-10, doi:10.1145/3581784.3627047.

Nakano, M., H. Yashiro, C. Kodama, and H. Tomita, 2018: Single precision in the dynamical core of a nonhydrostatic global atmospheric model: Evaluation using a baroclinic wave test case. *Mon. Wea. Rev.*, **146**, 409-416, doi:10.1175/MWR-D-17-0257.1.

Nishizawa, S., H. Yashiro, Y. Sato, Y. Miyamoto, and H. Tomita, 2015: Influence of grid aspect ratio on planetary boundary layer turbulence in large-eddy simulations. *Geosci. Model Dev.*, **8**, 3393-3419, doi:10.5194/gmd-8-3393-2015.

Palmer, T. N., 2001: A nonlinear dynamical perspective on model error: A proposal for non-local stochasticdynamic parametrization in weather and climate prediction models. *Q. J. R. Meteorol. Soc.*, **127**, 279–304.

Palmer, T.N., R. Buizza, F. Doblas-Reyes, T. Jung, M. Leutbecher, G.J. Shutts, M. Steinheimer, and A. Weisheimer, 2009: Stochastic parametrization and model uncertainty. *ECMWF Technical Memoranda*, **598**, 1-42.

Rüdisühli, S., A. Walser, and O. Fuhrer, 2014: COSMO in Single Precision. *COSMO*

Newsletter, **14**, 70-87, https://www.cosmo-model.org/content/model/documentation/newsLetters/newsLetter14/cnl14_09.pdf.

Sato, Y., S. Nishizawa, H. Yashiro, Y. Miyamoto, Y. Kajikawa, and H. Tomita, 2015: Impacts of cloud microphysics on trade wind cumulus: which cloud microphysics processes contribute to the diversity in a large eddy simulation? *Prog. Earth Planet. Sci.*, **2**, 23, doi:10.1186/s40645-015-0053-6.

Sueki, K., S. Nishizawa, T. Yamaura, and H. Tomita, 2022: Precision and convergence speed of the ensemble Kalman filter-based parameter estimation: estimating parameter uncertainty for reliable and efficient estimation. *Prog. Earth Planet. Sci.*, **9**, 47, doi:10.1186/s40645-022-00504-4.

Takano K., 2002: The application technique of ensemble forecasts. *Meteorological Research Note*, **201**, 73-103 (in Japanese).

Vána, F., P. Düben, S. Lang, T. Palmer, M. Leutbecher, D. Salmond, and G. Carver, 2017: Single precision in weather forecasting models: An evaluation with the IFS. *Mon. Wea. Rev.*, **145**, 495-502, doi:10.1175/MWR-D-16-0228.1.

Yamagishi, T., and Y. Matsumura, 2016: GPU acceleration of a non-hydrostatic ocean model with a multigrid Poisson/Helmholtz solver. *Procedia Computer Science*, **80**, 1658-1669, doi:10.1016/j.procs.2016.05.502.

Yamaura, T., S. Nishizawa, and H. Tomita, 2019: Theoretical time evolution of numerical errors when using floating point numbers in shallow-water models. *J. Adv. Model. Earth.*

Sy., doi:10.1029/2019MS001615.

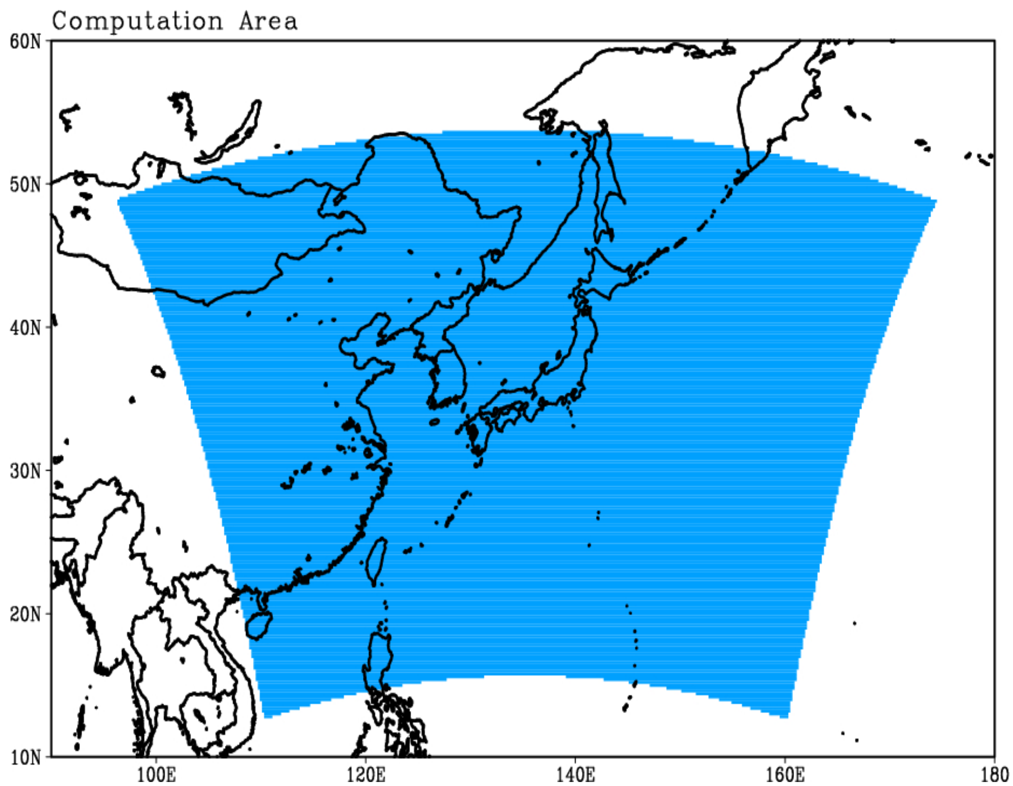

Fig. 1 Computational domain where SCALE-RM was performed in this study (shaded).

279x215mm (100 x 100 DPI)

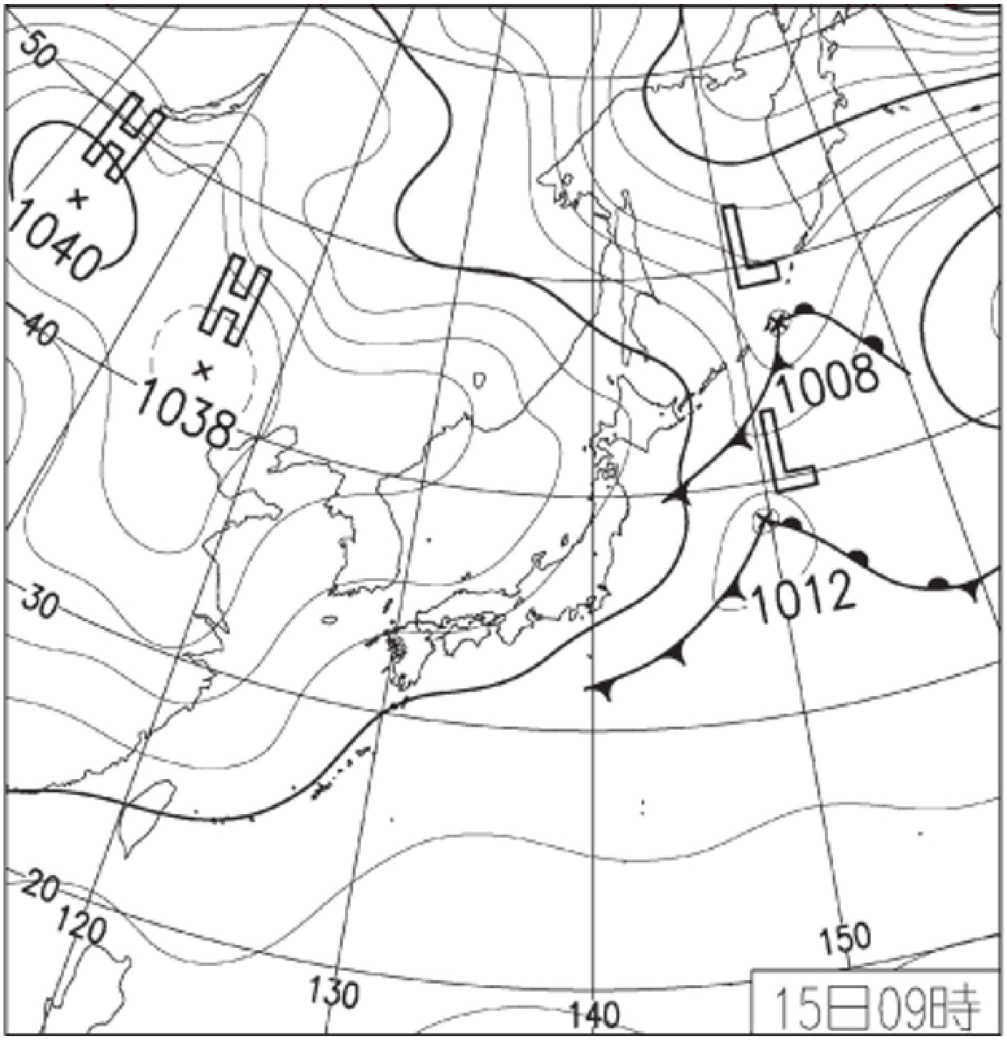

Fig. 2 Surface weather map around Japan at Oct 15, 2019.

430x444mm (37 x 37 DPI)

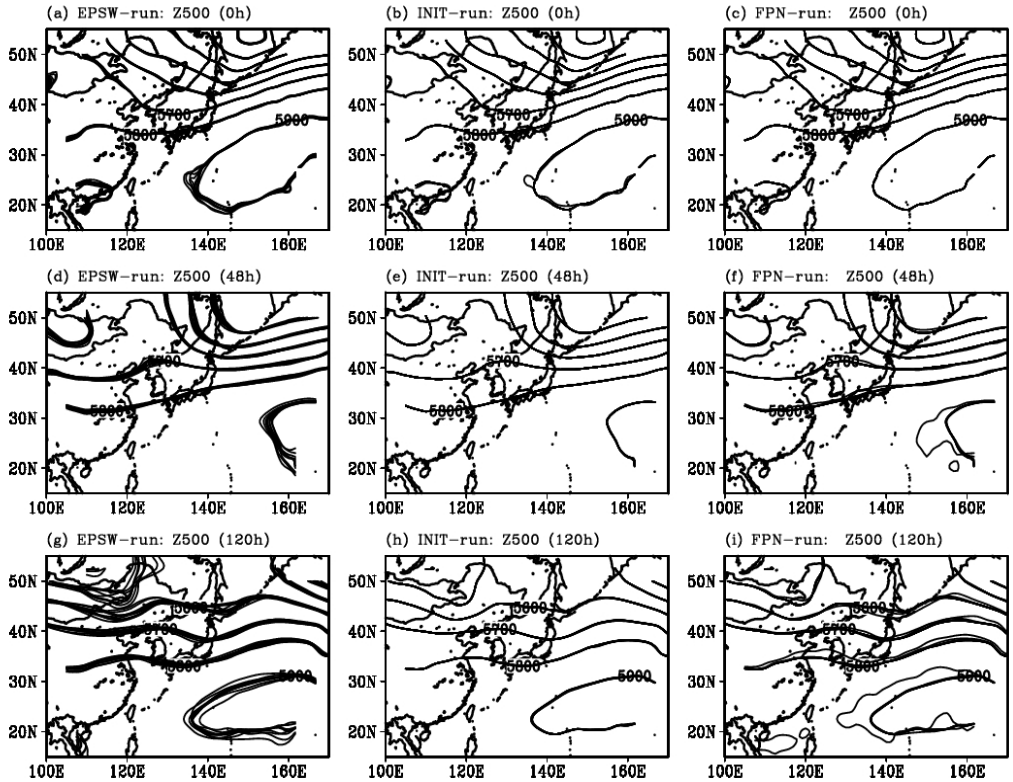

Fig. 3 Geopotential height at 500 hPa for the 5-day integration ensemble forecast experiment starting at 00 UTC on October 15, 2019. Contour intervals are 100 gpm; top row (a, b, c) represent initial time, middle row (d, e, f) represent 2 days after the start of integration, and bottom row (g, h, i) represent results from ensemble members 0 to 8 after 5 days of integration. The left column (a, d, g) shows the results of the EPSW-run, the middle column (b, e, h) the Init-run, and the right column (c, f, i) the FPN-run.

279x215mm (100 x 100 DPI)

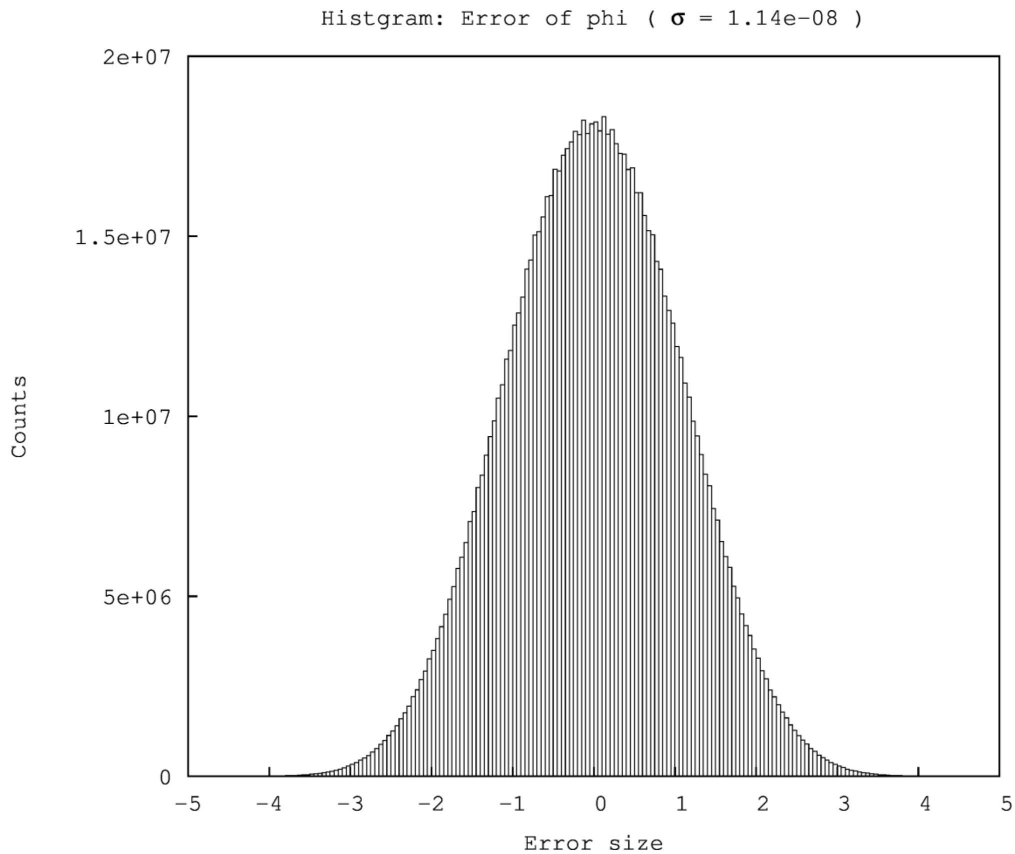

Fig. 4 Frequency distribution of the magnitude of rounding errors that occur during geostrophic wind equilibrium experiments based on Yamaura et al. (2019). The vertical axis shows the number of pieces and the horizontal axis shows the magnitude of the rounding error normalized by the standard deviation.

241x202mm (300 x 300 DPI)

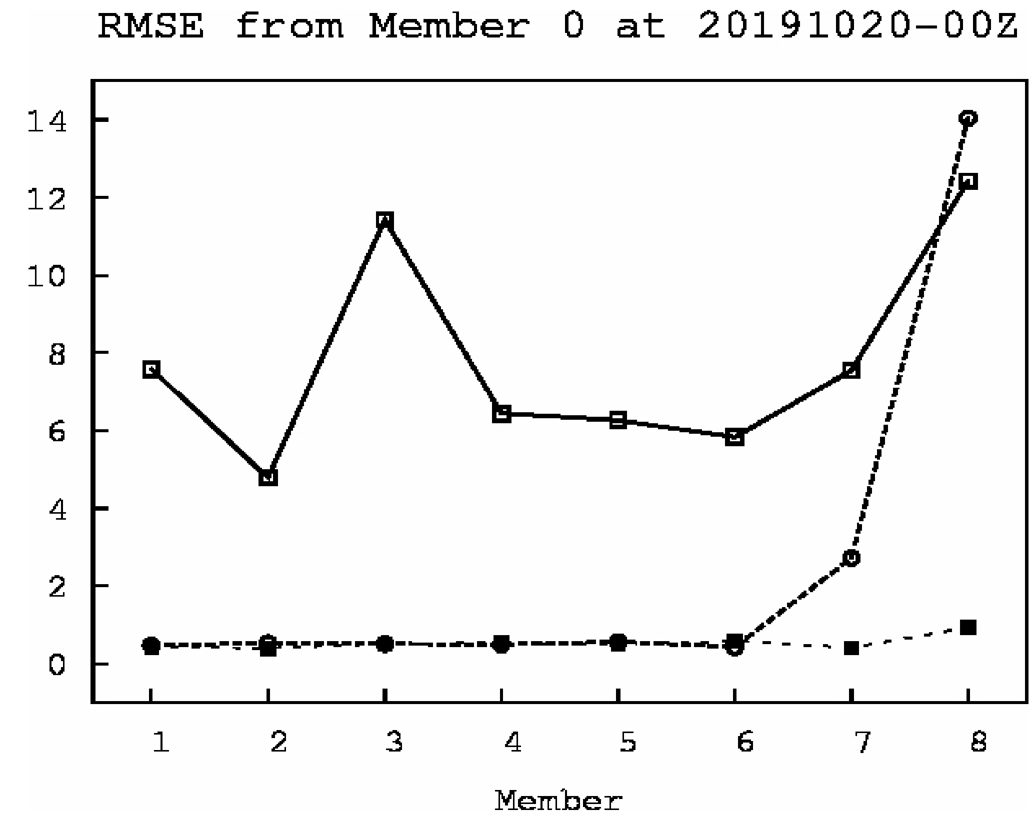

Fig. 5 RMSE with respect to ensemble member 0 after 5 days in a 5-day integration experiment starting at 00 UTC on October 15, 2019. The vertical axis represents the magnitude of the RMSE and the horizontal axis represents the member number. Solid lines indicate the results of the EPSW-run, dotted lines the results of the Init-run, and dashed lines the results of the FPN-run.

177x142mm (100 x 100 DPI)

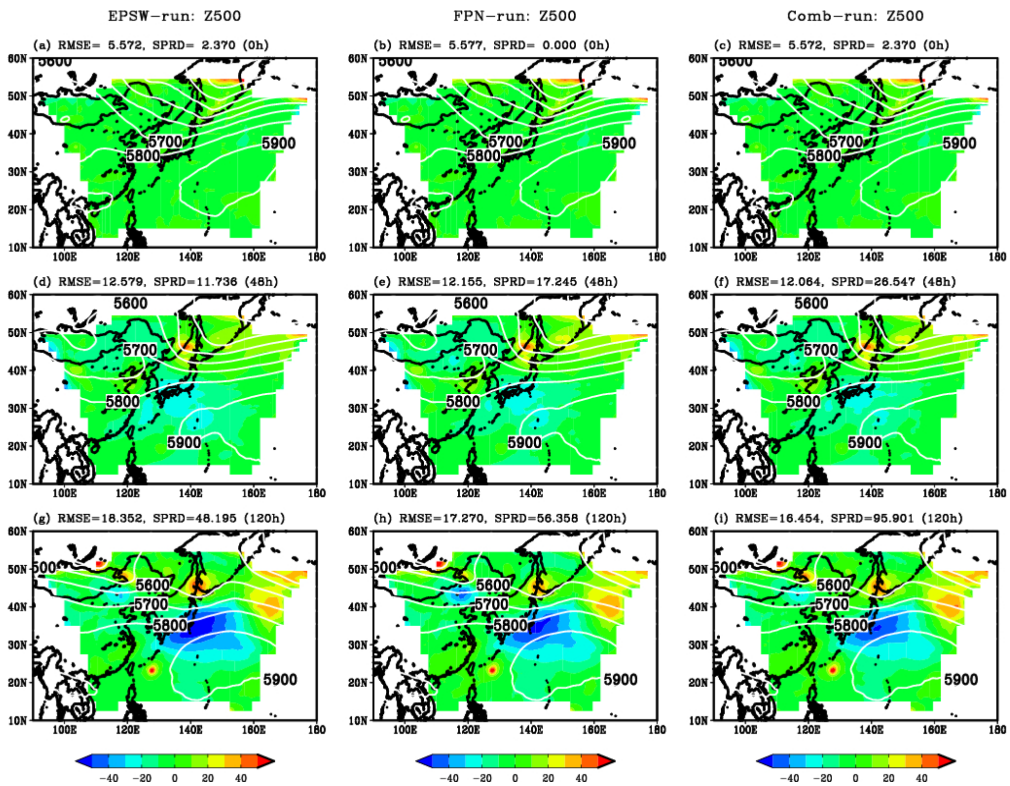

Fig. 6 Geopotential heights at 500 hPa for the 5-day integrated ensemble forecast experiment starting at 00 UTC on October 15, 2019. The contours show the results of objective analysis values from JMA-GPV at that time and are common in all figures. The contour interval is 100 gpm, and the shading indicates the difference of the ensemble mean from the objective analysis values. The top row (a, b, c) represents the initial time, the middle row (d, e, f) represents 2 days after the start of integration, and the bottom row (g, h, i) represents 5 days after the start of integration. The left columns (a, d, g) show the results of the EPSW-run, the middle columns (b, e, h) the FPN-run, and the right columns (c, f, i) the Comb-run. The RMSE and ensemble spread in each figure are listed at the top of the figure.

279x215mm (100 x 100 DPI)

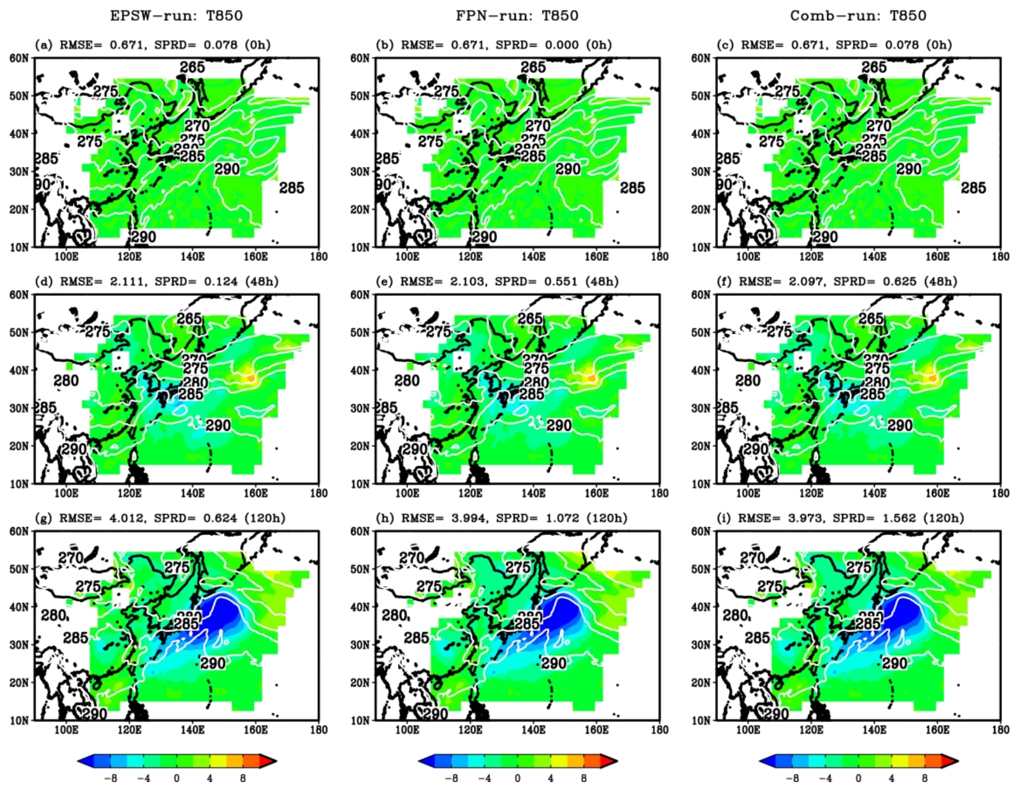

Fig. 7 Same as Figure 6, but for temperature at 850 hPa. The contour interval is 5 K.

279x215mm (300 x 300 DPI)

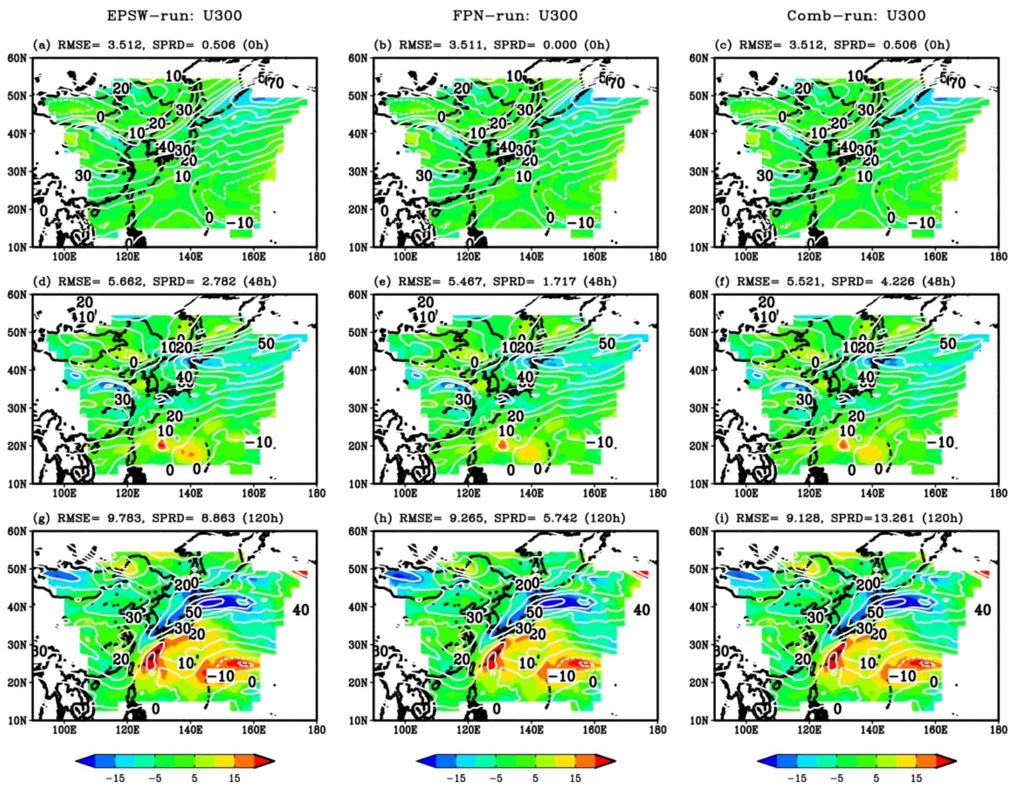

Fig. 8 Same as Figure 6, but for zonal winds at 300 hPa. The contour interval is 10 ms-1.

279x215mm (300 x 300 DPI)

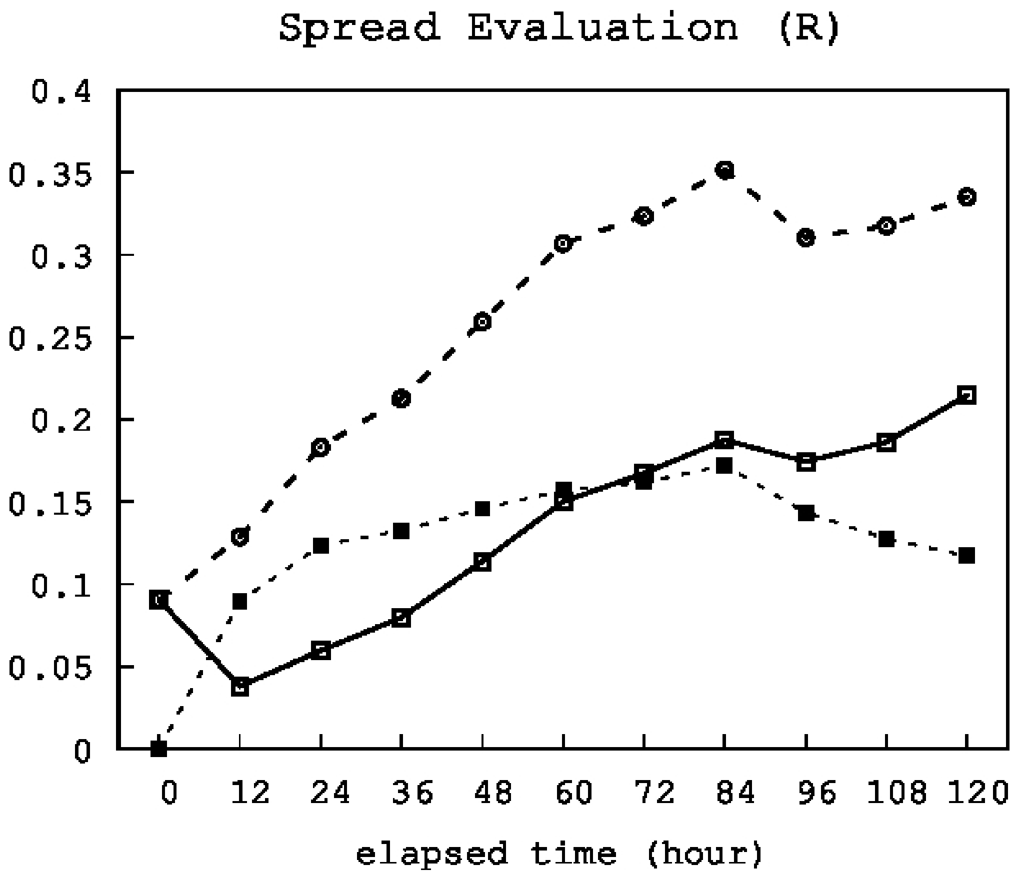

Fig. 9 Spread Evaluation Index (see text) evaluated in terms of geopotential height at 500 hPa from the start to the end of time integration for 24 cases with initial values at 00 UTC on the 1st and 15th of each month in 2019. The horizontal axis indicates elapsed time and the vertical axis indicates the magnitude of Spread Evaluation Index. Solid lines indicate results for the EPSW-run, dotted lines for the FPN-run, and dashed lines for the Comb-run.

154x133mm (100 x 100 DPI)

<table>
<tr><th>Ensemble Type</th><th colspan="2">Individual Ensemble</th><th>Give perturbations</th></tr>
<tr><td>Initial Value Ensemble</td><td rowspan="3">Multi-Model Ensemble</td><td>LAF</td><td>EnKF, LETKF, EOF, Local ET, BGM, SV</td></tr>
<tr><td>Model Ensemble</td><td>RP</td><td>SPPT, SKEB, STTP</td></tr>
<tr><td>Boundary Value Ensemble</td><td></td><td>SST perturbation</td></tr>
</table>

Table 1 Often using ensemble type for weather forecasting simulations (Japan Meteorological Agency 2016). Their respective abbreviations are as follows: Lagged-Average Forecasting (LAF), Random Parameter scheme (RP), Ensemble Kalman Filter (EnKF), Local Ensemble Transform Kalman Filter (LETKF), Empirical Orthogonal Function (EOF), Local Ensemble Transform (Local ET), Breeding Growth Mode (BGM), Singular Vector (SV), Stochastically Perturbed Parametrisation Tendencies (SPPT), Stochastic Kinetic Energy Backscatter (SKEB), Stochastic Total Tendency Perturbation (STTP).

576x118mm (59 x 59 DPI)